Journal of Molecular Liquids 414 (2024) 126248

Contents lists available at ScienceDirect

Journal of Molecular Liquids

journal homepage: www.elsevier.com/locate/molliq

Electrospinnability of PCL-doped eucalyptus kraft lignin and its application for structuring vegetable oils

José F. Rubio-Valle [a,*], Concepción Valencia [a], Giovanni Ferraro [b], M. Carmen Sánchez [a], José E. Martín-Alfonso [a], José M. Franco [a]

[a] Pro2TecS – Chemical Product and Process Technology Research Center, Department of Chemical Engineering and Materials Science, Universidad de Huelva, ETSI, Campus de "El Carmen", 21071 Huelva, Spain
[b] Department of Chemistry "Ugo Schiff" and CSGI, University of Florence, Via della Lastruccia 3-Sesto Fiorentino, I-50019 Florence, Italy

ARTICLE INFO

Keywords:
Electrospinning
Lignin
Rheology
Lubricant
Oleo-dispersion

ABSTRACT

This study explores the utilization of eucalyptus kraft lignin (EKL), extracted from black liquor of the pulp and paper industry, doped with polycaprolactone (PCL) to produce nanofibers with potential applications as vegetable oil structuring agents. Solutions of EKL:PCL in different weight ratios were prepared in a *N,N*-dimethylformamide/chloroform binary solvent, at concentrations ranging from 10 to 40 wt%, and submitted to electrospinning. Electrospinnability essentially correlates with the shear and extensional rheological properties of the solutions. Resulting electrospun EKL/PCL nanofibers were subsequently dispersed in castor oil at different concentrations (15 and 30 wt%). Stable gel-like dispersions were obtained with electrospun nanostructures predominantly composed of nanofibers or beaded fibers. The rheological properties and microstructure of EKL/PCL nanofiber-based oleo-dispersions were significantly influenced by both the EKL:PCL weight ratio and electrospun nanofiber concentration, with increases in the linear viscoelasticity functions and viscosity correlating with higher nanofiber concentrations and PCL proportions. These findings point out the potential of EKL/PCL nanofibers as eco-friendly vegetable oil structuring agents, in line with the principles of circular economy through the reuse of renewable waste materials.

1. Introduction

In recent decades, several strategies have been implemented to shift the economy toward a more sustainable use of renewable resources [1]. These approaches aim to promote more responsible natural resource management, decrease reliance on non-renewable energy sources, and address the challenges associated with climate change [2,3]. In this framework, the concept of the bioeconomy has emerged as an economic model that utilizes terrestrial, marine, and waste biological resources to drive both industrial and energy production, while integrating biological processes into sustainable industrial practices [4,5]. This perspective addresses the pressing need to protect the environment and confront the growing shortage of oil, leading some scientists to explore sustainable solutions [6]. For instance, in the field of lubrication, it is estimated that approximately 55 % of the volume of lubricants marketed each year ultimately contributes to environmental pollution [7]. This problem is aggravated by the complexity of the multi-component formulations of most lubricating greases available on the market, which consist mainly of non-biodegradable and non-renewable mineral or synthetic oils and thickeners, mostly based on lithium soaps [8]. The integration of bioeconomy approaches into lubricant technology aims not only to decrease dependence on non-renewable sources, but also to reduce the negative environmental impacts associated with the production and consumption of conventional lubricants [9,10].

The most relevant characteristics of conventional lubricating greases, typically classified in NLGI grades according to consistency or structuring level, are attributed to the microstructure generated by the thickener [11]. To date, considerable research has been undertaken to identify efficient and sustainable thickening or structuring agents for oil-based media. [12,13]. However, achieving appropriate compatibility of these biopolymers with vegetable oils often requires chemical modification, such as acetylation [14], methylation [15], ethylation [16], or acylation [17], to enhance their performance and stability in lubricant applications. Although the resulting formulations may be considered bio-based and non-toxic, the production processes require relatively complex chemical reactions and the utilization of chemicals and solvents

* Corresponding author.
E-mail address: josefernando.rubio@diq.uhu.es (J.F. Rubio-Valle).

https://doi.org/10.1016/j.molliq.2024.126248
Received 19 July 2024; Received in revised form 27 September 2024; Accepted 11 October 2024
Available online 18 October 2024

that are not environmentally friendly. Therefore, it is still necessary to find alternative cleaner processes and methods that avoid or reduce these chemical modifications. In this context, various vegetable oils such as sunflower, soybean and palm oils have been investigated as sustainable alternatives for lubricants [18–20]. However, castor oil (CO) stands out due to its high viscosity, superior lubricity and ability to form protective layers on metal surfaces, making it ideal for semi-solid lubricants [21,22]. In addition to being biodegradable and renewable, CO is widely available, cost effective and previously tested in lubricant and precision machining applications [23,24]. A simpler and greener approach to address the aforementioned shortcomings is to enhance the compatibility of biopolymers with oils through exclusively physical interactions [25,26]. The underlying hypothesis is that a structure consisting of micro- or nanometer-sized fibers with elevated porosity and surface-to-volume ratio could facilitate the formation of a three-dimensional percolation network within the oil medium [27,28]. In the field of nanofabrication, electrospinning stands out among other techniques such as force-spinning, melt-spinning, and solution-blown spinning because of its more feasible scalability at the industrial level [29]. The electrospinning technique offers the possibility of modifying the fiber morphology by adjusting various conditions, which can be divided into two main groups: solution-related factors and operating parameters [30]. Solution parameters include concentration, viscosity, polymer molecular weight, conductivity, surface tension, and solvent type [31,32]. This versatility enables the production of a broad range of nanostructures, encompassing particles, beaded fibers, smooth fibers, and ribbons, rendering them well-suited for diverse applications [33–36].

Within the wide selection of raw materials suitable for the electrospinning process, lignin emerges as a viable choice [37]. It is recognized as the second most plentiful natural polymer following cellulose, commonly found in plant cell walls, providing strength and rigidity [38]. Moreover, lignin is considered a byproduct of both the paper industry and the biofuel production derived from the lignocellulosic biomass [39–41]. Its use as a polymer for electrospinning offers a promising way to valorize these wastes, unveiling new application opportunities in different fields [42–44]. This not only helps to reduce dependence on fossil fuels and mitigate deforestation but also promotes sustainability by closing the life cycle of lignocellulosic products, thus advancing the principles of circular economy and environmental conservation [45]. Nonetheless, electrospinning lignin is somehow challenging due to its normally low molecular weight and complex and heterogeneous structure [46]. To overcome this limitation, the intervention of a dopant polymer is often necessary [47–49]. This additional polymer serves as a facilitator by increasing the entanglement density of lignin solutions, thus enhancing their ability to form fibers [50,51]. Several studies have explored different dopant polymers [52–54]. In particular, Ibarra et al. [55] reported the use of eucalyptus kraft lignins (EKL) obtained from different genotypes and precipitated at different pH doped with cellulose acetate. The utilization of polycaprolactone (PCL) as a dopant polymer is particularly noteworthy due to numerous and significant advantages, as it is a biodegradable and biocompatible polymer with excellent spinning properties [56,57].

In this work, electrospun fiber-bead EKL/PCL nanostructures are evaluated as structuring agents for castor oil. The electrospinnability of EKL solutions doped with PCL was investigated for the first time, and various types of nanostructures were obtained by modifying the solution concentration and EKL/PCL weight ratios. Further, the oil structuring ability of EKL/PCL nanostructures was assessed by determining the rheological properties of the resulting oleo-dispersions, which were related to their morphological attributes. The results herein shown reveal the potential of EKL/PCL nanofibers to replace traditional oil thickeners for different applications.

2. Material and methods

2.1. Materials

Eucalyptus lignin (EKL), obtained from the black liquor of a pulp mill in northern Spain using Kraft pulping, was kindly provided by INIA-CSIC (Madrid, Spain), and previously characterized as detailed elsewhere [58]. Polycaprolactone (PCL; M_w: 80,000 g/mol), *N,N*-dimethylformamide (DMF) and chloroform (Chl) were acquired from Merck Sigma-Aldrich (Darmstadt, Germany), whereas castor oil was acquired from Guinama (Valencia, Spain). The fatty acid composition and the primary physical characteristics of this vegetable oil can be found elsewhere [59].

2.2. Preparation and characterization of EKL/PCL solutions

EKL and EKL/PCL solutions with different concentrations (10, 20, 30, and 40 wt%) and EKL:PCL weight ratios (from 100:0 to 95:5 wt/wt) were prepared. Codes applied are shown in Table 1. These solutions were prepared using a solvent mixture of DMF/Chl (1:1 v/v). The preparation process involved stirring with a magnetic stirrer at 650 rpm for 24 h, at room temperature (22 °C).

EKL and EKL/PCL spinning solutions were subjected to physicochemical characterization, including surface tension, electrical conductivity, and shear and extensional viscosity measurements, which were performed at room temperature and in triplicate. Electrical conductivity was evaluated in a conductivity-meter (GLP 31, Crison, Spain) equipped with an immersion cell. The calibration of the conductivity-meter was performed using standard solutions of KCl within the suitable concentration range. Surface tension was determined using a surface tensiometer (Sigma 703D, Biolin Scientific, China) with a platinum Wilhelmy plate (39.24 mm wide × 0.1 mm thick). The shear viscosity measurements of the EKL and EKL/PCL solutions were conducted by implementing a stepped shear rate ramp ranging from 0.1 to 600 s^{-1} in a strain-controlled rotational rheometer (ARES Rheometric Scientific, UK) fitted with coaxial cylinders (inner diameter: 32 mm; length: 33.35 mm; gap:1 mm). The assessment of the extensional flow characteristics was carried out using a capillary break-up extensional rheometer (CaBER Haake, Thermo Scientific, Germany). This device is fitted with two plates, each 6 mm in diameter, initially separated by 1 mm. A fluid droplet was placed between the plates and subsequently stretched as the top plate ascended quickly. This prompts the formation of a filament which is influenced by viscous, elastic, and capillary forces. The variation in diameter at the filament's midpoint was measured using a laser micrometer with a 5 μm resolution, facilitating rapid data collection and allowing for high-speed measurements.

2.3. Electrospinning and characterization of EKL and EKL/PCL electrospun nanostructures

Electrospinning EKL and EKL/PCL solutions were conducted in a DOXA Microfluidics (Spain) chamber. A syringe filled with 10 ml of the spinning solution was employed and connected to an infusion pump, which regulated the flow rate in the range of 0.4–0.6 ml/h. A horizontal configuration was established, maintaining a distance of 10–12 cm between the collection plate and the needle tip (dimensions 21G). Electrical connections were established between the collection plate, the

Table 1
Nomenclature applied to EKL/PCL solutions.

Sample code	EKL (wt%)	PCL (wt%)
EKL100	100	0
EKL99-PCL1	99	1
EKL97-PCL3	97	3
EKL95-PCL5	95	5

capillary, and the high-voltage power supply, generating a potential difference of 12–15 kV. The experiments were conducted at room temperature and controlled relative humidity of 45 ± 1 %.

The morphology of electrospun nanostructures was analyzed in a JXA-8200 SuperProbe (JEOL ltd., Japan) microscope through Scanning Electron Microscopy (SEM), outfitted with a secondary electron detector that operates at an acceleration voltage of 15 kV. The samples due to their chemical nature presented limited conductivity so they required prior sputtering with gold [60] utilizing a sputter coating device BTT150 (HHV, UK). The analysis of the SEM images was carried out with the open-source software FIJI ImageJ using a plugin developed for this purpose called DiameterJ [61].

2.4. Preparation and characterization of EKL/PCL nanostructures dispersions in castor oil

The electrospun EKL/PCL nanostructures were gently removed from the collector plate using a pair of tweezers and a spatula. Selected nanostructures were dispersed in castor oil at 15 and 30 wt% concentrations, using an IKA RW-20 (Germany) mixer fitted with a low-shear anchor impeller. Fine dispersions were achieved by applying a protocol of 60 rpm rotational speed for 24 h at room temperature. The resulting oleo-dispersions were then allowed to stand for another 24 h for subsequent characterization.

Rheological characterization of oleo-dispersions was carried out at 25 °C, using a Rheoscope (TermoHaake, Karlsruhe, Germany) controlled-stress rheometer. A rough plate-and-plate geometry was used to mitigate potential slip phenomena (plate diameter: 20 mm, gap: 1 mm, relative roughness: 0.4). Small-amplitude oscillatory shear (SAOS) tests were performed in the linear viscoelastic range, spanning frequencies from 0.03 to 100 rad/s. Viscous flow measurements were also carried out in a range of shear rates from 0.01 to 100 s^{-1}. The morphology of the oleo-dispersions was evaluated using a Leica Stellaris 8 Falcon model laser scanning spectral confocal optical microscope, free spectral detection by AOBS: 410–850 nm, equipped with Leica HCX PL APO lambda blue 63× 1.4 hybrid oil objectives and detectors.

2.5. Statistical analysis

A statistical analysis was conducted on each of the parameters evaluated. This analysis involved a one-factor variance analysis (ANOVA), with three independent replications of each measurement, which allows the calculation of various statistical parameters, including the mean and standard deviation. Furthermore, a test comparing means was executed to identify any significant differences ($p < 0.05$).

3. Results and discussion

3.1. Physicochemical properties of EKL/PCL spinning solutions

As previously highlighted and documented in numerous studies [43,62,63], the electrospinnability of a polymer solution is inherently connected to both the electrospinning process parameters and the physicochemical properties of the spinning solution, specifically surface tension, electrical conductivity, and viscosity [64,65]. These properties and process parameters are influenced by the nature of the polymer, the solvents employed, and the concentration of the polymer in the spinning solution [31,33]. Table 2 presents the surface tension, electrical conductivity, and dynamic and extensional viscosity data of the EKL/PCL solutions used in this study to feed the spinning chamber as a function of concentration and EKL:PCL weight ratio. It is observed that the surface tension values, ranging from 27.71 to 33.75 mN/m, increase with EKL/PCL concentration and decrease as the PCL proportion increases. These results are consistent with previous studies on the spinnability of lignin doped with other polymers [66,67] and may be ascribed to the polar character of lignin, which confers a marked affinity for the solvents

Table 2
Surface tension (σ), electrical conductivity (Λ), shear (η) and extensional (η_{ext}) viscosities, and relaxation time (λ) of EKL:PCL solutions in 1:1 v/v DMF:Chl mixture.

Concentration (wt%)	EKL: PCL ratio	σ (mN/m)	Λ (μS/cm)	η (mPa.s)	$\eta_{ext,0}$ (mPa.s)	λ (ms)
10	100:0	29.65^{a}	190.1^{A}	19.9^{aa}	57.6^{AA}	–
	99:1	29.55^{a}	185.2^{B}	21.5^{aa}	61.1^{AA}	–
	97:3	28.32^{b}	184.3^{B}	29.6^{bb}	91.5^{BB}	–
	95:5	27.71^{c}	178.9^{C}	51.1^{cc}	148.9^{CC}	12.1^{α}
20	100:0	31.34^{d}	191.1^{A}	24.4^{aa}	74.7^{DD}	–
	99:1	29.77^{a}	188.5^{C}	39.9^{dd}	123.4^{EE}	13.3^{α}
	97:3	28.75^{b}	185.1^{B}	79.2^{ee}	236.5^{FF}	21.2^{β}
	95:5	28.15^{b}	165.3^{D}	156.5^{ff}	470.4^{GG}	49.9^{γ}
30	100:0	31.91^{d}	196.6^{E}	49.4^{cc}	146.2^{CC}	–
	99:1	30.01^{e}	191.7^{A}	70.1^{ee}	208.8^{HH}	30.7^{δ}
	97:3	29.44^{a}	168.4^{D}	187.6^{gg}	592.5^{II}	95.8^{ε}
	95:5	28.85^{b}	129.5^{F}	416.9^{hh}	1179.7^{JJ}	185.8^{φ}
40	100:0	33.75^{f}	197.3^{E}	72.2^{ee}	210.3^{HH}	15.6^{α}
	99:1	31.19^{d}	175.7^{C}	132.6^{ii}	336.1^{KK}	45.4^{γ}
	97:3	30.91^{e}	145.3^{G}	313.4^{jj}	920.3^{LL}	128.2^{φ}
	95:5	30.06^{e}	91.5^{H}	920.9^{kk}	2817.5^{MM}	245.1^{χ}

Values on the same column differing in their superscripts were significantly different ($p < 0.05$).

used, resulting in increased cohesion and consequently higher surface tension [49,55]. Surface tension favors the formation of nanofibers, due to the enhanced cohesive forces that facilitate the stretching of the liquid within the capillary, preventing the formation of droplets [31]. Besides, the electrical conductivity of spinning solutions containing a higher proportion of PCL was lower than those containing only EKL. Moreover, the electrical conductivity initially increased with the spinning solution concentration, reached a maximum value at a given concentration which depends on the EKL:PCL weight ratio, and then gradually decreased. This decrease is consistent with previous research [32], which investigated the influence of solution properties on the electrospinning process of various cellulose derivatives. This phenomenon is due to the decreased movement of intertwined macromolecules once they exceed the overlap concentration threshold [50,68].

Fig. 1a shows the viscosity versus shear rate plots for EKL/PCL spinning solutions prepared at 40 wt% as a function of EKL:PCL weight ratio, while Fig. 1b collects the shear viscosity data of all the spinning solutions examined. As can be observed, all solutions studied exhibited a Newtonian response within the shear rate range applied. An increase in shear viscosity is observed as the EKL/PCL concentration increases, while the viscosity decreases as the proportion of EKL increases. This phenomenon is explained by the interactions between the EKL and PCL molecules, where higher PCL contents result in greater flow resistance due to the higher molecular weight and intermolecular bonds, yielding an increased entanglement density [27,47,69]. These results are consistent with those of other authors, especially Oroumei et al. [70], who investigated the electrospinnability of a hardwood organosolv lignin. They created submicron fiber mats from a broad spectrum of polymer solutions with varying ratios of organosolv lignin and polyacrylonitrile (PAN) and different concentrations. In general, solution viscosity, which reflects the degree of polymer entanglement, is emerging as a critical factor of fiber formation during the electrospinning process [71]. Several studies have established correlations between different ranges of polymer concentration and typical fiber structures, such as beaded fibers and homogeneous smooth fibers [33,43]. Numerous authors have investigated the relationship between the viscosity of the solution and polymer concentration and identified several concentration regimes ranging from dilute to concentrated,

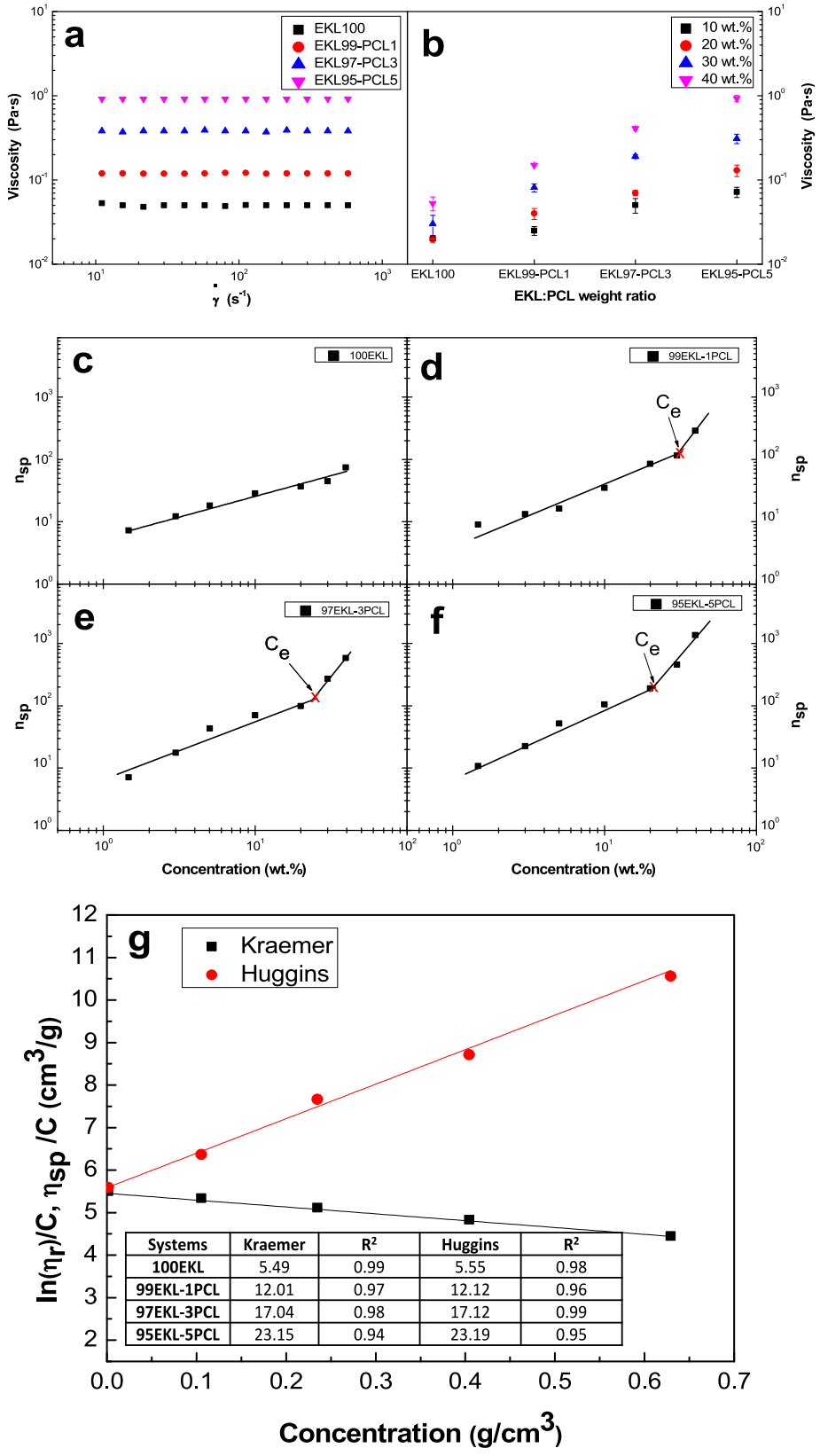

Fig. 1. (a) Shear viscosity vs. shear rate plots for 40 wt% solutions and variable EKL:PCL ratios; (b) values of shear viscosity for all EKL/PCL spinning solutions; (c, d, e, and f) specific viscosity vs. EKL/PCL concentration plots and estimation of the critical entanglement concentration (C_e) in EKL/PCL spinning solutions; and (e) Kraemer and Huggins plots for EKL solutions, with intrinsic viscosity values for all EKL/PCL solutions shown in the inset.

including both entangled and non-entangled semi-dilute states [50,51]. Fig. 1c–f display the correlation between the specific viscosity (η_{sp},) and polymer concentration for the different EKL:PCL weight ratios. The critical entanglement concentration (C_e), indicating the transition from the non-entangled semi-dilute and entangled semi-dilute regimes, can be calculated by the intersection of lines with different slopes [72]. As can be seen, Fig. 1c basically shows one linear trend with a slope value associated with the non-entangled semi-dilute regime. This was to be expected for the PCL-free solutions, i.e. prepared exclusively with EKL. On the other hand, Fig. 1d-f, corresponding to the EKL99-PCL1, EKL97-PCL3, and EKL95-PCL5 systems, respectively, depict varying C_e, which decreases with increasing PCL concentration. Approximate C_e values obtained were 31.2, 25.7, and 20.5 wt%, respectively. For $C > C_e$, an increment of the scaling exponent was observed, going from $\eta_{sp} \sim C^{1.1\text{-}1.5}$ to $\eta_{sp} \sim C^{3.1\text{-}3.5}$, in accordance with the corresponding values predicted for neutral polymers in a suitable solvent [73]. C_e is crucial for assessing the electrospinnability of polymeric solutions and for predicting the resulting electrospun structures' morphology [32]. It has been suggested that the concentration of the spinning solution should be at least 2–2.5 times the C_e [33], underscoring its significance. Furthermore, these experimental results strongly support the previous hypothesis regarding the reduction of macromolecular mobility when discussing the effects of solution concentration and EKL:PCL weight ratio on electrical conductivity, which was found at a concentration that fairly well matches the transition to the semidilute entangled regime.

To gain deeper insights into polymer–solvent interactions, the intrinsic viscosity [η] was estimated. As well-known, the intrinsic viscosity reflects the capacity of macromolecules to increase the solution viscosity without intermolecular interactions [74]. The Kraemer and Huggins models are the most commonly used methods for predicting [η] [75]. Fig. 1g shows how the intrinsic viscosity of the EKL100 system was extrapolated as the Y-intercept, corresponding to zero concentration [47]. Both models exhibited a fairly satisfactory fit to the measured data, providing similar [η] values ranging between 5.49 and 5.55 cm^3/g. The intrinsic viscosity values for solutions prepared with varying EKL:PCL weight ratios are also included in the inset table (Fig. 1g). As can be seen, a higher PCL proportion leads to higher [η] values. Intrinsic viscosity is recognized for its ability to offer an understanding of the interactions between the individual polymer and the solvent, as well as the polymer's specific hydrodynamic volume or average molecular weight [76]. High [η] values indicate compact EKL/PCL structures in the DMF/Chl with strong solvent interactions [50], suggesting good compatibility. Finally, the [η] can be correlated with C_e, which helps to validate the accuracy of the rheological measurements performed. According to Graessley [77], who proposed a relationship between [η] and the overlap concentration (C*) derived from the De Gennes reptation theory, C* is assumed to be $0.77/[\eta]$, whereas $C_e \approx 10$ C*. Using these expressions, C_e values of 32.7, 25.6, and 20.4 wt% are predicted for the EKL99-PCL1, EKL97-PCL3, and EKL95-PCL5 systems, respectively, which are very similar to those obtained empirically in Fig. 1d–f.

The extensional viscosity of the EKL/PCL solutions was investigated by capillary breakage experiments. The filament thinning profiles for several EKL95-PCL5 concentrations are presented in Fig. 2a. Once the filament was created at t = 0, the diameter at the midpoint, D(t), was measured using a laser micrometer and recorded as a function of time. The evolution of D(t) was normalized with the initial filament diameter, D_0. For EKL/PCL concentrations lower than 20 wt%, measuring D(t) was challenging due to sudden filament breakages or no filament formation, whereas at higher concentrations more stable filaments with exponentially decreasing diameters were observed. This pattern aligns with previous findings [47,66]; noteworthy are the studies of Dallmeyer et al. [48]. They encountered challenges in filament formation within solutions containing solely lignin at low weight concentrations, indicating a threshold viscosity below which filament formation is hindered. In the case of EKL:PCL solutions prepared at 30 and 40 wt% with high EKL/PCL weight ratios, an almost linear thinning of the filaments was observed,

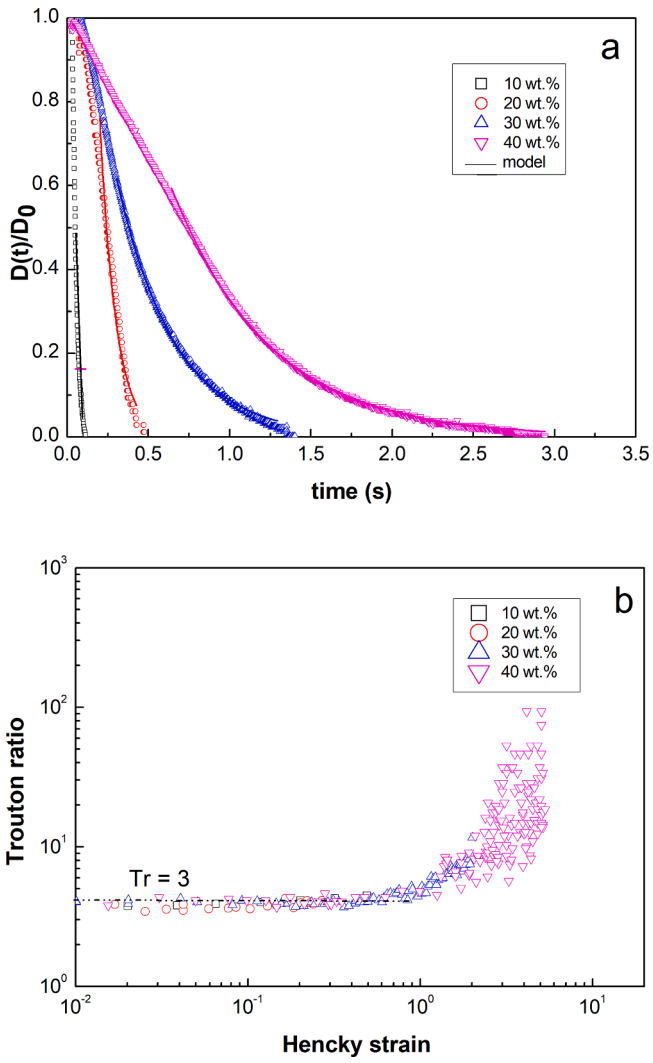

Fig. 2. Extensional flow properties of EKL95-PCL5 solutions at different polymer concentrations: (a) evolution of filament diameter with time; and (b) Trouton ratio versus Hencky strain.

which is characteristic of pure Newtonian fluids. Conversely, a characteristic exponential reduction in filament diameter, typically found in viscoelastic fluids, was noted at lower EKL:PCL weight ratios, as shown in Fig. 2a. Rodd et al. proposed a functional model to fit the evolution of D(t) (Eq. (1)) as a function of the solution characteristic relaxation time (λ) [78].

$$\frac{D(t)}{D_0} = A \bullet e^{(-t/3\lambda)} = \left(\frac{GD_0}{2\sigma}\right)^{1/3} \bullet e^{(-t/3\lambda)} \quad (1)$$

where G is the elastic modulus. Table 2 shows the λ values obtained by fitting Eq. (1) to the experimental data. The relaxation time increases with the solution concentration and PCl proportion, varying from 12.1 ms for the system prepared with 10 wt% EKL95-PCL5 to 245.1 ms for the system prepared with 40 wt% EKL95-PCL5. Numerous studies have emphasized the impact of λ on the electrospinning process [27,33,66]. In addition to this, the extensional viscosity was determined as follows [79]:

$$\eta_{ext} = \frac{\sigma}{\frac{-d(D(t))}{dt}} \quad (2)$$

Fig. 2b represents the extensional viscosity of EKL95-PCL5 solutions in the form of the Trouton ratio (η_{ext}/η) versus the Hencky strain (ε),

defined as [80]:

$$\varepsilon = -2ln\left(\frac{D(t)}{D_0}\right) \quad (3)$$

Table 2 lists the values of the short-limiting extensional viscosity ($\eta_{ext,0}$). The extensional viscosity of these solutions stayed fairly constant over time during the early stages of the tests and later significantly increased as the extensional deformation increased [80,81]. In general, the extensional viscosity increased with both the spinning solution concentration and the PCL proportion, as a result of the enhanced viscoelastic character. As seen in Fig. 2b, the theoretical value of the Trouton ratio (around 3) predicted for low strains (or low stretching times) was fulfilled in all cases over a wide deformation range, and then the Trouton ratio experienced a notable increase over time, particularly in the case of more concentrated spinning solutions. These results underscore the importance of conducting extensional and shear viscosity tests to evaluate the electrospinnability of polymer solutions. While shear tests reveal both Newtonian and non-Newtonian behaviors, extensional experiments encompass the viscoelastic character and filament stability, which can be crucial in the process of electrospinning as discussed below.

3.2. Electrospinnability of EKL/PCL solutions

Fig. 3 shows the morphological characteristics of electrospun EKL/PCL nanostructures obtained by SEM as a function of the spinning solution concentration and EKL:PCL weight ratio. As can be seen, the solutions prepared with 10 wt% of the EKL/PCL blend did not produce interconnected nanofibers regardless of the EKL:PCL ratio, resulting in a physical electrospray of particles instead of a electrospinning (Fig. 3a, e and i). By increasing the concentration of the solutions up to 20 wt%, micro- and nanometer-sized particles eventually connected by thin filaments (of approximately 90 nm diameter) were obtained (Fig. 3b, f and j), to a greater extent for the EKL95-PCL5 system. Particles embedded in a nanofiber mat and/or beaded fibers were observed when increasing EKL/PCL concentration up to 30 wt% for the lower EKL:PCL weight ratios (Fig. 3g and k). In addition, the fiber diameter of the EKL95-PCL5 system increased significantly compared to that obtained with the 20 wt % spinning solution (from 130 nm to 310 nm). Finally, beaded nanofiber mats were obtained from 40 wt% solutions in all systems containing PCL (Fig. 3d, h and i), with larger particles as the PCL proportion decreases. On the contrary, the average fiber diameter increased with PCL content in the electrospinning solution, from 240 nm to 680 nm.

As above mentioned, the different morphologies obtained depend on the physicochemical properties of the spinning solutions. According to Fig. 1c–f, solutions in the semi-dilute non-entangled regime essentially produced particles or aggregates of particles, while solutions in the semi-dilute entangled regime with concentrations close to the estimated C_e yielded beaded fibers or fibers interconnecting particles. Finally, it is confirmed that solutions with concentrations higher than 2–2.5 times C_e produced more uniform nanofiber mats. In addition, these results are consistent with the minimum relaxation times previously reported for successful electrospinning [28,82].

In this case, λ values of around 45 ms are required to see the transition from structures essentially formed by micro- or nano-particles to nanofibers connecting nanoparticles. Higher λ values (of around 100–245 ms) are needed to maintain stable the spinning process and achieve nanostructures predominantly composed of nanofibers.

In general, more uniform fiber mats and thicker fibers were obtained by increasing the solution concentration and lowering the EKL:PCL weight ratio. Fig. 4 shows two empirical relationships between the specific viscosity and relaxation time versus the mean fiber diameter of EKL/PCL spinning solutions. As can be seen, in both cases, the specific viscosity and relaxation time follow a potential evolution with the average fiber diameter, having power-law exponents of 1.5 and 1.2, respectively. According to this, the architecture of electrospun

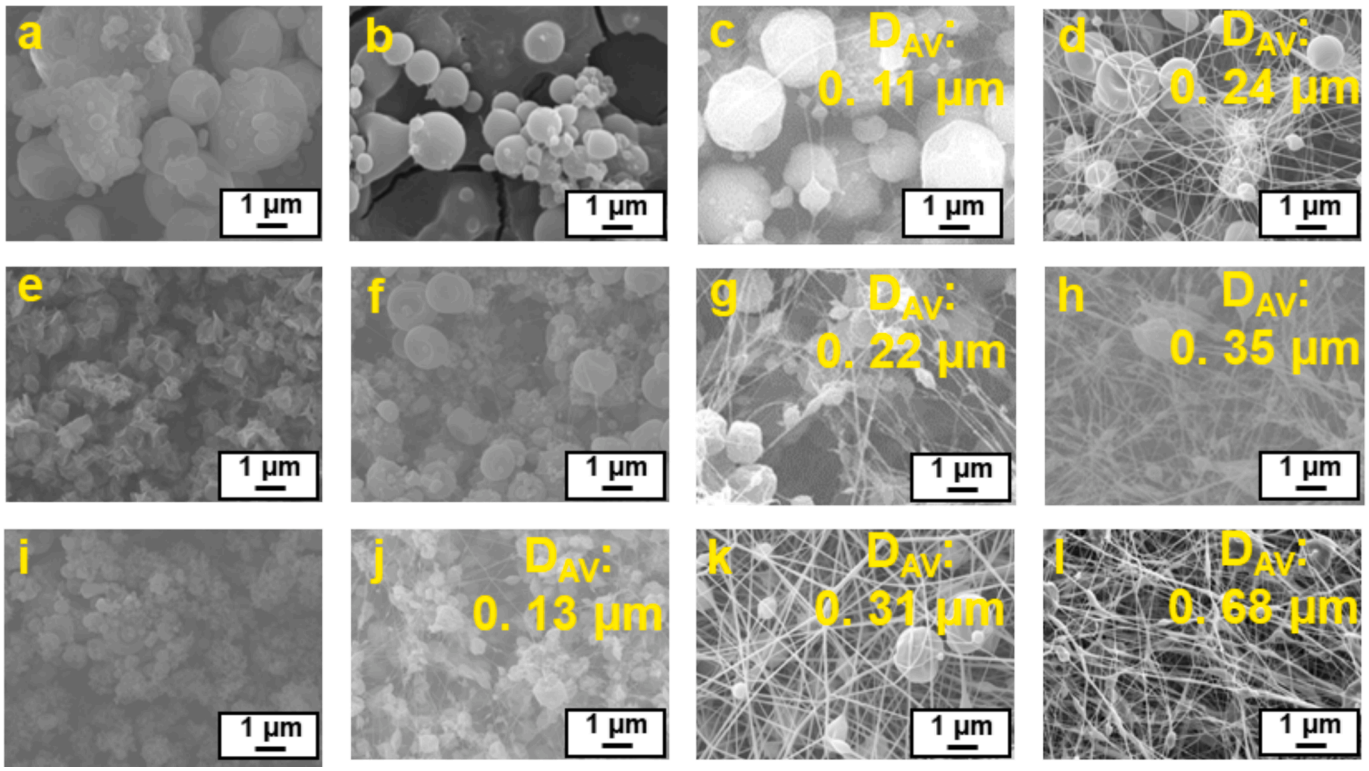

Fig. 3. SEM images of electrospun nanostructures obtained from solutions with varying concentrations and EKL:PLC ratio: (a) EKL99-PCL1 at 10 wt%; (b) EKL99-PCL1 at 20 wt%; (c) EKL99-PCL1 at 30 wt%; (d) EKL99-PCL1 at 40 wt%; (e) EKL97-PCL3 at 10 wt%; (f) EKL97-PCL3 at 20 wt%; (g) EKL97-PCL3 at 30 wt%; (h) EKL97-PCL3 at 40 wt%; (i) EKL95-PCL5 at 10 wt%; (j) EKL95-PCL5 at 20 wt%; (k) EKL95-PCL5 at 30 wt%; and (l) EKL95-PCL5 at 40 wt%.

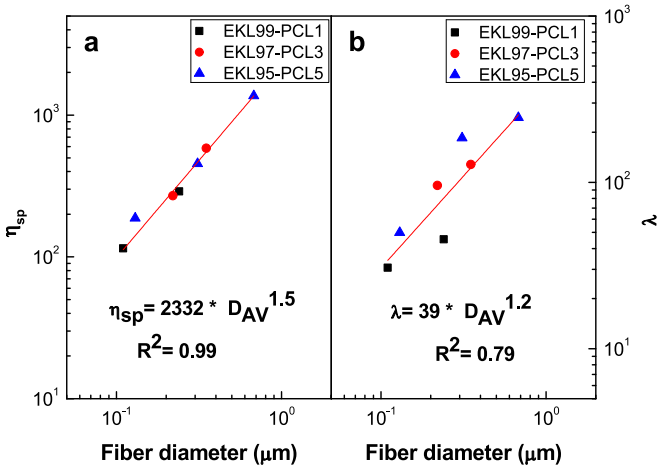

Fig. 4. Correlations between (a) the specific viscosity; and (b) the relaxation timeof EKL/PCL spinning solutions and the average diameter (D_{AV}) of electrospun nanofibers.

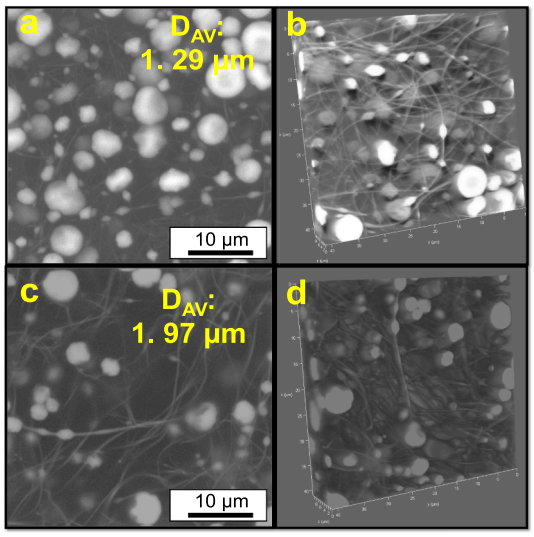

Fig. 5. Micrographs of the oleo-dispersions obtained with (a, b) EKL97-PCL3; and (c, d) EKL95-PCL5 electrospun nanostructures (spinning solution concentration: 40 wt%).

nanostructures is essentially dependent on the rheological properties of the spinning solution, with the effect of electrical conductivity and surface tension being marginal, at least in the experimental ranges studied.

3.3. Capability of EKL/PCL electrospun nanostructures for oil structuring

According to previous research [10,66], only electrospun nanostructures consisting of well-established uniform nanofiber mats, or at least beaded nanofibers, can develop stable gel-like systems when dispersed in castor oil. In contrast, nanostructures composed of particles obtained by electrospraying, such as those obtained with EKL100 solution, result in unstable dispersions that lead to oil separation. This discrepancy is explained by the enhanced stabilization promoted by nanofibers achieved through physical interactions, mainly hydrophobic and van der Waals intermolecular forces [27,67], which allows the entrapment of the oil within the three-dimensional network. Therefore, the formation of nanofiber mats by electrospinning is crucial for the generation of stable dispersions due to the high specific surface area and aspect ratio [26,83]. This premise was initially confirmed in previous studies [26,47] and subsequently validated by other researchers such as Valoppi et al. [25], who have pioneered the development of oleogels based on the oil structuring ability of lipid nanofibers with potential applications for replacing solid fats in the food, cosmetics, and pharmaceutical industries.

The gentle dispersion of nanofiber mats in castor oil does not significantly alter the morphological properties of the electrospun nanostructures. Fig. 5 presents confocal microscopy images illustrating the microstructure of electrospun nanostructures once dispersed in castor oil. As can be seen, the EKL97-PCL3 nanostructure, derived from 40 wt% spinning solutions, exhibits a rather heterogeneous morphology in which embedded particles or beaded fibers can eventually be observed (Fig. 5a and b). In contrast, the oleo-dispersion formulated with EKL95-PCL5, obtained from a spinning solution at a concentration of 40 wt%, shows a regular network predominantly composed of fibers (Fig. 5c and d). The only effect observed when the nanofibers are dispersed in oil is a noticeable swelling. Therefore, the diameter of the particles and fibers within the percolation network increases significantly, a phenomenon consistently observed for nanofibers prepared with different PCL proportion.

The oil structuring capacity of electrospun nanostructures derived from EKL was also evaluated by means of rheological tests. The rheological characteristics of EKL/PCL oleo-dispersions are significantly affected by the morphological properties of the electrospun nanostructures, which in turn depend on both the spinning solution concentration and the EKL:PCL ratio, as discussed above. Fig. 6a, b and c display the evolution of the SAOS functions (specifically, storage modulus (G′), loss modulus (G″), and loss tangent (G″/G′)) with frequency for oleo-dispersions obtained by dispersing 15 and 30 wt% electrospun EKL97-PCL3 and EKL95-PCL5 nanostructures in castor oil. As can be observed, all the oleo-dispersions display mechanical spectra that are remarkably similar, characteristic of colloidal dispersions [27,67], where G′ values surpass those of G″ across a broad frequency spectrum with low-frequency dependency, while G″ approaches a minimum. This mechanical spectrum is indicative of the packing density achieved within the fiber network of electrospun fibers [84]. The main distinction lies in the magnitude of G' and G", which increase by almost one order of magnitude with both the PCL proportion and the electrospun nanostructure concentration. As shown in Fig. 6a and b, the values of G′ range from around 10^2 to 10^4 Pa, depending on the electrospun nanostructure used and its concentrations, while the values of G″ are roughly one order of magnitude lower. However, interestingly, the relative elastic character (i.e., the loss tangent) does not show significant differences (Fig. 6c).

Fig. 6d displays the viscous flow curves, of the oleo-dispersions formulated with the electrospun EKL/PCL nanofibers. Over the entire range of experimental shear rates investigated, a consistent shear-thinning response was observed in all cases. This shear-thinning behavior is adequately described by the power-law model ($R^2 > 0.905$):

$$\eta = K \bullet \dot{\gamma}^{n-1} \quad (4)$$

where K and n are the consistency and flow indices, respectively. Table 3 shows the K and n values obtained by fitting the data to Eq. (4). Consistent with the aforementioned influence observed in the SAOS functions, increasing nanofiber concentration and PCL proportion resulted in higher viscosity and, therefore, higher K values. Moreover, a more pronounced shear thinning behavior, i.e. lower n values, was found when increasing nanofiber concentration or PCL content. Overall, the rheological properties of the resulting oleo-dispersions are influenced by the morphology of the electrospun nanoarchitectures, which can be fine-tuned by adjusting the concentration of the spinning solution and/or the EKL:PCL weight ratio. Finally, it is noteworthy that the rheological behavior of oleo dispersions containing 30 wt% nanofibers is very similar to that reported for conventional lubricating greases [33,85].

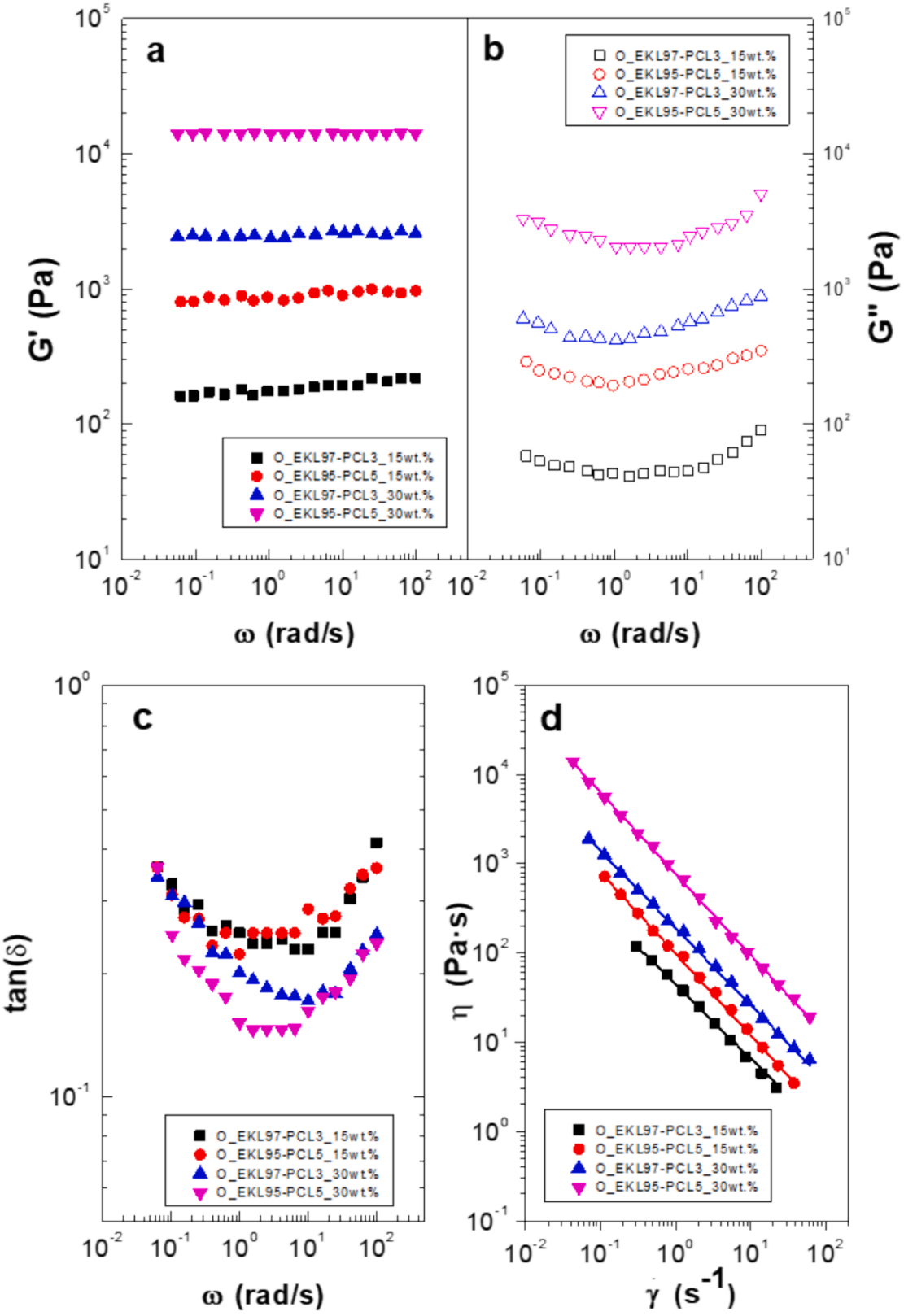

Fig. 6. Influence of the concentration and EKL:PCL weight ratio on the rheological properties of electrospun nanofiber oleo-dispersions: evolutions of (a) the storage modulus (G′); (b) the loss modulus (G″); (c) the loss tangent as a function of frequency; and (d) viscosity versus shear rate plots. Viscosity data were fitted to the power-law model (Eq. (4)). (Spinning solution concentration: 40 wt%).

Table 3
Values of the consistency and flow indices of oleo-dispersions prepared with different concentrations of electrospun nanofibers differing in the EKL: PCLweight ratio.

Oleo-dispersions*	K(Pa·s^n)**	n(–)**
O_EKL97-PCL3_15 wt%	45.06^a	0.21^A
O_EKL95-PCL5_15 wt%	96.43^b	0.11^B
O_EKL97-PCL3_30 wt%	191.84^c	0.12^B
O_EKL95-PCL5_30 wt%	717.84^d	0.06^C

* Nanofibers obtained from spinning solutions at 40 wt% concentration.
** Values on the same column differing in their superscripts were significantly different ($p < 0.05$).

4. Concluding remarks

Solutions of eucalyptus kraft lignin (EKL) doped with small amounts of polycaprolactone (PCL), in a 1:1 v/v *N,N*-dimethylformamide/chloroform solvent mixture, show variable electrospinning performance, depending on the solution concentration and EKL:PCL weight ratio. Electrospinnability mainly correlates with shear and extensional rheological properties of the solutions, resulting in a more successful production of nanofibers with larger average diameters as specific viscosity and relaxation time increase.

Oleo-dispersions were obtained by dispersing electrospun nanofiber mats in castor oil at different concentrations (15 and 30 wt%). Electrospun nanostructures predominantly composed of nanofibers, or at least beaded nanofibers, produced stable gel-like dispersions in castor oil. In contrast, nanostructures composed of particles, such as those obtained from PCL-free EKL spinning solutions, resulted in unstable dispersions. The rheological response and microstructure of electrospun EKL/PCL nanofiber-based oleo-dispersions were significantly affected by both the EKL:PCLweight ratio and the nanofiber concentration. The linear viscoelasticity functions and viscosity values of the resulting oleo-dispersions increase with nanofiber concentration and PCL proportion.

In addition, the rheological behavior of castor oil structures with EKL/PCL electrospun nanofibers showed similarities with conventional lubricating greases. This suggests that EKL-based nanostructures derived from pulp mill black liquor have the potential to replace conventional oil thickeners in the lubricant, contributing to the circular economy paradigm. In this respect, further work is required to thoroughly study the lubrication performance of these systems.

CRediT authorship contribution statement

José F. Rubio-Valle: Writing – original draft, Software, Methodology, Investigation, Formal analysis, Data curation, Conceptualization. **Concepción Valencia:** Writing – review & editing, Visualization, Resources, Formal analysis, Data curation, Investigation. **Giovanni Ferraro:** Investigation, Resources. **M. Carmen Sánchez:** Validation, Data curation, Investigation. **José E. Martín-Alfonso:** Visualization, Validation, Resources, Formal analysis, Investigation, Writing – review & editing. **José M. Franco:** Writing – review & editing, Visualization, Validation, Supervision, Resources, Project administration, Methodology, Funding acquisition, Investigation.

Declaration of competing interest

The authors declare that they have no known competing financial interests or personal relationships that could have appeared to influence the work reported in this paper.

Acknowledgements

This work was part of Research Project PID2021-125637OB-I00, funded by MCIN/AEI/10.13039/501100011033 and by "ERDF A way of making Europe". J.F. Rubio-Valle additionally received a PhD Research Grant PRE2019-090632 from Spain's Ministry of Science and Innovation. All funding is gratefully acknowledged. Open Access funding provided by Universidad de Huelva / CBUA, thanks to the CRUE-CSIC agreement with Elsevier.

Data availability

Data will be made available on request.

References

[1] Q. Hassan, P. Viktor, T.J. Al-Musawi, B. Mahmood Ali, S. Algburi, H.M. Alzoubi, A. Khudhair Al-Jiboory, A. Zuhair Sameen, H.M. Salman, M. Jaszczur, The renewable energy role in the global energy transformations, Renew. Energy Focus 48 (2024) 100545, https://doi.org/10.1016/j.ref.2024.100545.
[2] M. Sadiq, K. Chavali, V.V.A. Kumar, K.-T. Wang, P.T. Nguyen, T.Q. Ngo, Unveiling the relationship between environmental quality, non-renewable energy usage and natural resource rent: fresh insights from ten asian economies, Resour. Policy 85 (2023) 103992, https://doi.org/10.1016/j.resourpol.2023.103992.
[3] C. Yu, M. Moslehpour, T.K. Tran, L.M. Trung, J.P. Ou, N.H. Tien, Impact of non-renewable energy and natural resources on economic recovery: empirical evidence from selected developing economies, Resour. Policy 80 (2023) 103221, https://doi.org/10.1016/j.resourpol.2022.103221.
[4] C. Patermann, A. Aguilar, The origins of the bioeconomy in the European Union, New Biotechnol. 40 (2018) 20–24, https://doi.org/10.1016/j.nbt.2017.04.002.
[5] V. Ferreira, L. Pié, A. Mainar-Causapé, A. Terceño, The bioeconomy in Spain as a new economic paradigm: the role of key sectors with different approaches, Environ. Dev. Sustain. 26 (2023) 3369–3393, https://doi.org/10.1007/s10668-022-02830-5.
[6] O.N. Anand, V.K. Chhibber, Vegetable oil derivatives: environment-friendly lubricants and fuels, J. Synth. Lubr. 23 (2006) 91–107, https://doi.org/10.1002/jsl.14.
[7] A.Z. Syahir, N.W.M. Zulkifli, H.H. Masjuki, M.A. Kalam, A. Alabdulkarem, M. Gulzar, L.S. Khuong, M.H. Harith, A review on bio-based lubricants and their applications, J. Clean. Prod. 168 (2017) 997–1016, https://doi.org/10.1016/j.jclepro.2017.09.106.
[8] T.M. Panchal, A. Patel, D.D. Chauhan, M. Thomas, J.V. Patel, A methodological review on bio-lubricants from vegetable oil based resources, Renew. Sustain. Energy Rev. 70 (2017) 65–70, https://doi.org/10.1016/j.rser.2016.11.105.
[9] A. Aguilar, T. Twardowski, R. Wohlgemuth, Bioeconomy for sustainable development, Biotechnol. J. 14 (2019), https://doi.org/10.1002/biot.201800638.
[10] J.F. Rubio-Valle, C. Valencia, M.C. Sánchez, J.E. Martín-Alfonso, J.M. Franco, Upcycling spent coffee grounds and waste PET bottles into electrospun composite nanofiber mats for oil structuring applications, Resour. Conserv. Recycl. 199 (2023) 107261, https://doi.org/10.1016/j.resconrec.2023.107261.
[11] National Lubricating Grease Institute, NLGI Lubricating Greases Guide, fifth edition, Kansas City, MO, USA, 2006.
[12] A.M. Borrero-López, F.J. Santiago-Medina, C. Valencia, M.E. Eugenio, R. Martin-Sampedro, J.M. Franco, Valorization of kraft lignin as thickener in castor oil for lubricant applications, J. Renew. Mater. 6 (2018) 347–361, https://doi.org/10.7569/JRM.2017.634160.
[13] E. Cortés-Triviño, C. Valencia, M.A. Delgado, J.M. Franco, Rheology of epoxidized cellulose pulp gel-like dispersions in castor oil: influence of epoxidation degree and the epoxide chemical structure, Carbohydr. Polym. 199 (2018) 563–571, https://doi.org/10.1016/j.carbpol.2018.07.058.
[14] M. Trejo-Cáceres, M.C. Sánchez, J.E. Martín-Alfonso, Impact of acetylation process of kraft lignin in development of environment-friendly semisolid lubricants, Int. J. Biol. Macromol. 227 (2023) 673–684, https://doi.org/10.1016/j.ijbiomac.2022.12.096.
[15] J.E. Martín Alfonso, R. Yañez, C. Valencia, J.M. Franco, M.J. Díaz, Optimization of the methylation conditions of kraft cellulose pulp for its use as a thickener agent in biodegradable lubricating greases, Ind. Eng. Chem. Res. 48 (2009) 6765–6771, https://doi.org/10.1021/ie9002766.
[16] J.E. Martín-Alfonso, N. Núñez, C. Valencia, J.M. Franco, M.J. Díaz, Formulation of new biodegradable lubricating greases using ethylated cellulose pulp as thickener agent, J. Ind. Eng. Chem. 17 (2011) 818–823, https://doi.org/10.1016/j.jiec.2011.09.003.
[17] R. Sánchez, G. Alonso, C. Valencia, J.M. Franco, Rheological and TGA study of acylated chitosan gel-like dispersions in castor oil: influence of acyl substituent and acylation protocol, Chem. Eng. Res. Des. 100 (2015) 170–178, https://doi.org/10.1016/j.cherd.2015.05.022.
[18] A review on eco-friendly green biolubricants from renewable and sustainable plant oil sources, Biointerface Res. Appl. Chem. 11 (2021) 13303–13327, doi: 10.33263/BRIAC115.1330313327.
[19] M.A. Martín-Alfonso, J.F. Rubio-Valle, J.P. Hinestroza, J.E. Martín-Alfonso, Impact of vegetable oil type on the rheological and tribological behavior of montmorillonite-based oleogels, Gels 8 (2022) 504, https://doi.org/10.3390/gels8080504.
[20] J.F. Rubio-Valle, C. Valencia, M.C. Sánchez-Carrillo, J.E. Martín-Alfonso, J. M. Franco, Valorization of kraft lignins from different poplar genotypes as vegetable oil structuring agents via electrospinning for biolubricant applications,

ACS Sustain. Chem. Eng. 12 (2024) 12260–12269, https://doi.org/10.1021/acssuschemeng.4c05013.
[21] M.C. Dwivedi, S. Sapre, Total vegetable-oil based greases prepared from castor oil, J. Synth. Lubr. 19 (2002) 229–241, https://doi.org/10.1002/jsl.3000190305.
[22] Q. Zeng, The lubrication performance and viscosity behavior of castor oil under high temperature, Green Mater. 10 (2022) 51–58, https://doi.org/10.1680/jgrma.20.00068.
[23] H.J. Pei, Y.J. Shen, C.G. Shen, G.C. Wang, Application of castor oil-based cutting fluids in precision turning, Appl. Mech. Mater. 130–134 (2011) 3830–3834, https://doi.org/10.4028/www.scientific.net/AMM.130-134.3830.
[24] S. Guo, C. Li, Y. Zhang, Y. Wang, B. Li, M. Yang, X. Zhang, G. Liu, Experimental evaluation of the lubrication performance of mixtures of castor oil with other vegetable oils in MQL grinding of nickel-based alloy, J. Clean. Prod. 140 (2017) 1060–1076, https://doi.org/10.1016/j.jclepro.2016.10.073.
[25] F. Valoppi, J. Schavikin, P. Lassila, I. Laidmäe, J. Heinämäki, S. Hietala, E. Haeggström, A. Salmi, Formation and characterization of oleogels obtained via direct dispersion of ultrasound-enhanced electrospun nanofibers and cold milling, Food Struct. 37 (2023) 100338, https://doi.org/10.1016/j.foostr.2023.100338.
[26] M. Borrego, J.E. Martín-Alfonso, C. Valencia, M.C. Sánchez Carrillo, J.M. Franco, Developing electrospun ethylcellulose nanofibrous webs: an alternative approach for structuring castor oil, ACS Appl. Polym. Mater. 4 (2022) 7217–7227, https://doi.org/10.1021/acsapm.2c01090.
[27] M.A. Martín-Alfonso, J.F. Rubio-Valle, J.E. Martín-Alfonso, J.M. Franco, Oleo-dispersions of electrospun cellulose acetate butyrate nanostructures: toward renewable semisolid lubricants, Adv. Sustain. Syst. (2024), https://doi.org/10.1002/adsu.202300592.
[28] J.F. Rubio-Valle, C. Valencia, M. Sánchez, J.E. Martín-Alfonso, J.M. Franco, Oil structuring properties of electrospun Kraft lignin/cellulose acetate nanofibers for lubricating applications: influence of lignin source and lignin/cellulose acetate ratio, Cellulose 30 (2023) 1553–1566, https://doi.org/10.1007/s10570-022-04963-2.
[29] Y. Liu, M. Hao, C. Zhou, B. Yang, S. Jiang, J. Huang, Z. Chen, Y. Liu, S. Ramakrishna, Scale-up strategies for electrospun nanofiber production, in: Electrospun Nanofibrous Membr., Elsevier, 2023, pp. 205–266, https://doi.org/10.1016/B978-0-12-823032-9.00020-9.
[30] V. Pillay, C. Dott, Y.E. Choonara, C. Tyagi, L. Tomar, P. Kumar, L.C. du Toit, V.M. K. Ndesendo, A review of the effect of processing variables on the fabrication of electrospun nanofibers for drug delivery applications, J. Nanomater. 2013 (2013) 1–22, https://doi.org/10.1155/2013/789289.
[31] J.F. Rubio-Valle, M. Jiménez-Rosado, V. Perez-Puyana, A. Guerrero, A. Romero, Electrospun nanofibres with antimicrobial activities, in: Antimicrob. Text. from Nat. Resour., Elsevier, 2021, pp. 589–618, doi: 10.1016/B978-0-12-821485-5.00020-2.
[32] P. Sánchez-Cid, J.F. Rubio-Valle, M. Jiménez-Rosado, V. Pérez-Puyana, A. Romero, Effect of solution properties in the development of cellulose derivative nanostructures processed via electrospinning, Polymers (Basel) 14 (2022) 665, https://doi.org/10.3390/polym14040665.
[33] M.A. Martín-Alfonso, J.E. Martín-Alfonso, J.F. Rubio-Valle, J.P. Hinestroza, J. M. Franco, Tunable architectures of electrospun cellulose acetate phthalate applied as thickeners in green semisolid lubricants, Appl. Mater. Today 36 (2024) 102030, https://doi.org/10.1016/j.apmt.2023.102030.
[34] A.M. Mohammed, M.R. Thalji, S.A. Yasin, J.-J. Shim, K.F. Chong, A.A. Guda, G.A. M. Ali, Recent advances in electrospun fibrous membranes for effective chromium (VI) removal from water, J. Mol. Liq. 383 (2023) 122110, https://doi.org/10.1016/j.molliq.2023.122110.
[35] S. Aslanzadeh, B. Ahvazi, Y. Boluk, C. Ayranci, Morphologies of electrospun fibers of lignin in poly(ethylene oxide)/N, N-dimethylformamide, J. Appl. Polym. Sci. 133 (2016), https://doi.org/10.1002/app.44172.
[36] L. Prazeres Mazur, R. Reis Ferreira, R. Felix da Silva Barbosa, P. Henrique Santos, T. Barcelos da Costa, M. Gurgel Adeodato Vieira, A. da Silva, D. dos Santos Rosa, L. Helena Innocentini Mei, Development of novel biopolymer membranes by electrospinning as potential adsorbents for toxic metal ions removal from aqueous solution, J. Mol. Liq. 395 (2024) 123782, https://doi.org/10.1016/j.molliq.2023.123782.
[37] I. Dallmeyer, F. Ko, J.F. Kadla, Electrospinning of technical lignins for the production of fibrous networks, J. Wood Chem. Technol. 30 (2010) 315–329, https://doi.org/10.1080/02773813.2010.527782.
[38] G. Gellerstedt, G. Henriksson, Lignins: major sources, structure and properties, in: Monomers, Polym. Compos. from Renew. Resour., Elsevier, 2008, pp. 201–224, doi: 10.1016/B978-0-08-045316-3.00009-0.
[39] J. Rencoret, A. Gutiérrez, E. Castro, J.C. del Río, Structural characteristics of lignin in pruning residues of olive tree (Olea europaea L.), Holzforschung 73 (2018) 25–34, https://doi.org/10.1515/hf-2018-0077.
[40] C. Fajardo, A. Blánquez, G. Domínguez, A.M. Borrero-López, C. Valencia, M. Hernández, M.E. Arias, J. Rodríguez, Assessment of sustainability of bio treated lignocellulose-based oleogels, Polymers (Basel) 13 (2021) 267, https://doi.org/10.3390/polym13020267.
[41] P. Manzanares, E. Ruiz, M. Ballesteros, M.J. Negro, F.J. Gallego, J.C. López-Linares, E. Castro, Residual biomass potential in olive tree cultivation and olive oil industry in Spain: valorization proposal in a biorefinery context, Span. J. Agric. Res. 15 (2017) e0206, https://doi.org/10.5424/sjar/2017153-10868.
[42] S. Aslanzadeh, B. Ahvazi, Y. Boluk, C. Ayranci, Carbon fiber production from electrospun sulfur free softwood lignin precursors, J. Eng. Fiber. Fabr. 12 (2017) 155892501701200, https://doi.org/10.1177/155892501701200405.
[43] M. Borrego, J.E. Martín-Alfonso, C. Valencia, M.C. Sánchez, J.M. Franco, Impact of the morphology of electrospun lignin/ethylcellulose nanostructures on their capacity to thicken castor oil, Polymers (Basel) 14 (2022) 4741, https://doi.org/10.3390/polym14214741.
[44] E. Cortés-Triviño, J. Cubero-Cardoso, A. Tenorio-Alfonso, M.A. Fernández-Recamales, C. Valencia, J. Urbano, J.M. Franco, Structuring natural deep eutectic solvents with epoxidised lignin-enriched residues: a green alternative to petroleum-based thickened formulations, J. Mol. Liq. 360 (2022) 119433, https://doi.org/10.1016/j.molliq.2022.119433.
[45] A.M. Borrero-López, C. Valencia, J.M. Franco, Lignocellulosic materials for the production of biofuels, biochemicals and biomaterials and applications of lignocellulose-based polyurethanes: a review, Polymers (Basel) 14 (2022) 881, https://doi.org/10.3390/polym14050881.
[46] J. Rencoret, G. Marques, A. Gutiérrez, D. Ibarra, J. Li, G. Gellerstedt, J.I. Santos, J. Jiménez-Barbero, Á.T. Martínez, J.C. del Río, Structural characterization of milled wood lignins from different eucalypt species, Holzforschung 62 (2008), https://doi.org/10.1515/HF.2008.096.
[47] J.F. Rubio-Valle, M.C. Sánchez, C. Valencia, J.E. Martín-Alfonso, J.M. Franco, Electrohydrodynamic processing of PVP-doped Kraft lignin micro- and nano-structures and application of electrospun nanofiber templates to produce oleogels, Polymers (Basel) 13 (2021) 2206, https://doi.org/10.3390/polym13132206.
[48] I. Dallmeyer, F. Ko, J.F. Kadla, Correlation of elongational fluid properties to fiber diameter in electrospinning of softwood kraft lignin solutions, Ind. Eng. Chem. Res. 53 (2014) 2697–2705, https://doi.org/10.1021/ie403724y.
[49] L. García-Fuentevilla, J.F. Rubio-Valle, R. Martín-Sampedro, C. Valencia, M. E. Eugenio, D. Ibarra, Different Kraft lignin sources for electrospun nanostructures production: influence of chemical structure and composition, Int. J. Biol. Macromol. 214 (2022) 554–567, https://doi.org/10.1016/j.ijbiomac.2022.06.121.
[50] S.L. Shenoy, W.D. Bates, H.L. Frisch, G.E. Wnek, Role of chain entanglements on fiber formation during electrospinning of polymer solutions: good solvent, non-specific polymer–polymer interaction limit, Polymer (Guildford) 46 (2005) 3372–3384, https://doi.org/10.1016/j.polymer.2005.03.011.
[51] L. Kong, G.R. Ziegler, Role of molecular entanglements in starch fiber formation by electrospinning, Biomacromolecules 13 (2012) 2247–2253, https://doi.org/10.1021/bm300396j.
[52] S. Aslanzadeh, Z. Zhu, Q. Luo, B. Ahvazi, Y. Boluk, C. Ayranci, Electrospinning of colloidal lignin in poly(ethylene oxide) N,N-dimethylformamide solutions, Macromol. Mater. Eng. 301 (2016) 401–413, https://doi.org/10.1002/mame.201500317.
[53] S. Devadas, S.M.N. Al-Ajrash, D.A. Klosterman, K.M. Crosson, G.S. Crosson, E. S. Vasquez, Fabrication and characterization of electrospun poly(acrylonitrile-co-methyl acrylate)/lignin nanofibers: effects of lignin type and total polymer concentration, Polymers (Basel) 13 (2021) 992, https://doi.org/10.3390/polym13070992.
[54] J. Wang, L. Tian, B. Luo, S. Ramakrishna, D. Kai, X.J. Loh, I.H. Yang, G.R. Deen, X. Mo, Engineering PCL/lignin nanofibers as an antioxidant scaffold for the growth of neuron and Schwann cell, Colloids Surf. B Biointerfaces 169 (2018) 356–365, https://doi.org/10.1016/j.colsurfb.2018.05.021.
[55] D. Ibarra, L. García-Fuentevilla, J.F. Rubio-Valle, R. Martín-Sampedro, C. Valencia, M.E. Eugenio, Kraft lignins from different poplar genotypes obtained by selective acid precipitation and their use for the production of electrospun nanostructures, React. Funct. Polym. 191 (2023) 105685, https://doi.org/10.1016/j.reactfunctpolym.2023.105685.
[56] L. Gritsch, L. Liverani, C. Lovell, A.R. Boccaccini, Polycaprolactone electrospun fiber mats prepared using benign solvents: blending with copper(II)-chitosan increases the secretion of vascular endothelial growth factor in a bone marrow stromal cell line, Macromol. Biosci. 20 (2020), https://doi.org/10.1002/mabi.201900355.
[57] V. Perez-Puyana, M. Jiménez-Rosado, A. Guerrero, A. Romero, Anisotropic properties of PCL/gelatin scaffolds obtained via electrospinning, Int. J. Fract. 224 (2020) 269–276, https://doi.org/10.1007/s10704-020-00460-4.
[58] C. Fernández-Costas, S. Gouveia, M.A. Sanromán, D. Moldes, Structural characterization of Kraft lignins from different spent cooking liquors by 1D and 2D Nuclear Magnetic Resonance spectroscopy, Biomass Bioenergy 63 (2014) 156–166, https://doi.org/10.1016/j.biombioe.2014.02.020.
[59] L.A. Quinchia, M.A. Delgado, C. Valencia, J.M. Franco, C. Gallegos, Viscosity modification of different vegetable oils with EVA copolymer for lubricant applications, Ind. Crop. Prod. 32 (2010) 607–612, https://doi.org/10.1016/j.indcrop.2010.07.011.
[60] Stokroos, Kalicharan, Van Der Want, Jongebloed, A comparative study of thin coatings of Au/Pd, Pt and Cr produced by magnetron sputtering for FE-SEM, J. Microsc. 189 (1998) 79–89, https://doi.org/10.1046/j.1365-2818.1998.00282.x.
[61] N.A. Hotaling, K. Bharti, H. Kriel, C.G. Simon, DiameterJ: a validated open source nanofiber diameter measurement tool, Biomaterials 61 (2015) 327–338, https://doi.org/10.1016/j.biomaterials.2015.05.015.
[62] I. Dallmeyer, L.T. Lin, Y. Li, F. Ko, J.F. Kadla, Preparation and characterization of interconnected, kraft lignin-based carbon fibrous materials by electrospinning, Macromol. Mater. Eng. 299 (2014) 540–551, https://doi.org/10.1002/mame.201300148.
[63] N. Bhardwaj, S.C. Kundu, Electrospinning: a fascinating fiber fabrication technique, Biotechnol. Adv. 28 (2010) 325–347, https://doi.org/10.1016/j.biotechadv.2010.01.004.
[64] G.K. Celep, K. Dincer, Optimization of parameters for electrospinning of polyacrylonitrile nanofibers by the taguchi method, Int. Polym. Proc. 32 (2017) 508–514, https://doi.org/10.3139/217.3411.
[65] C. Salas, Solution electrospinning of nanofibers, in: Electrospun Nanofibers, Elsevier, 2017, pp. 73–108, doi: 10.1016/B978-0-08-100907-9.00004-0.

[66] M. Borrego, J.E. Martín-Alfonso, M.C. Sánchez, C. Valencia, J.M. Franco, Electrospun lignin-PVP nanofibers and their ability for structuring oil, Int. J. Biol. Macromol. 180 (2021) 212–221, https://doi.org/10.1016/j.ijbiomac.2021.03.069.
[67] J.F. Rubio-Valle, J.E. Martín-Alfonso, M.E. Eugenio, D. Ibarra, J.M. Oliva, P. Manzanares, C. Valencia, Bioethanol lignin-rich residue from olive stones for electrospun nanostructures development and castor oil structuring, Int. J. Biol. Macromol. 255 (2024) 128042, https://doi.org/10.1016/j.ijbiomac.2023.128042.
[68] O. Hosseinaei, D.P. Harper, J.J. Bozell, T.G. Rials, Role of physicochemical structure of organosolv hardwood and herbaceous lignins on carbon fiber performance, ACS Sustain. Chem. Eng. 4 (2016) 5785–5798, https://doi.org/10.1021/acssuschemeng.6b01828.
[69] P. Gupta, C. Elkins, T.E. Long, G.L. Wilkes, Electrospinning of linear homopolymers of poly(methyl methacrylate): exploring relationships between fiber formation, viscosity, molecular weight and concentration in a good solvent, Polymer (Guildford) 46 (2005) 4799–4810, https://doi.org/10.1016/j.polymer.2005.04.021.
[70] A. Oroumei, B. Fox, M. Naebe, Thermal and rheological characteristics of biobased carbon fiber precursor derived from low molecular weight organosolv lignin, ACS Sustain. Chem. Eng. 3 (2015) 758–769, https://doi.org/10.1021/acssuschemeng.5b00097.
[71] S. Wu, Chain structure and entanglement, J. Polym. Sci. B 27 (1989) 723–741, https://doi.org/10.1002/polb.1989.090270401.
[72] H. Nie, A. He, J. Zheng, S. Xu, J. Li, C.C. Han, Effects of chain conformation and entanglement on the electrospinning of pure alginate, Biomacromolecules 9 (2008) 1362–1365, https://doi.org/10.1021/bm701349j.
[73] R.H. Colby, Structure and linear viscoelasticity of flexible polymer solutions: comparison of polyelectrolyte and neutral polymer solutions, Rheol. Acta 49 (2010) 425–442, https://doi.org/10.1007/s00397-009-0413-5.
[74] S.H. Maron, R.B. Reznik, A new method for determination of intrinsic viscosity, J. Polym. Sci. Part A-2 Polym. Phys. 7 (1969) 309–324, https://doi.org/10.1002/pol.1969.160070206.
[75] R.D. Sudduth, Development of Huggins' and Kraemer's equations for polymer solution evaluations from the generalized viscosity model for suspensions, J. Appl. Polym. Sci. 66 (1997) 2319–2332, https://doi.org/10.1002/(SICI)1097-4628(19971219)66:12<2319::AID-APP13>3.0.CO;2-V.
[76] R. Pamies, J.G. Hernández Cifre, M. del Carmen López Martínez, J. García de la Torre, Determination of intrinsic viscosities of macromolecules and nanoparticles. Comparison of single-point and dilution procedures, Colloid Polym. Sci. 286 (2008) 1223–1231, https://doi.org/10.1007/s00396-008-1902-2.
[77] W. Graessley, Polymer chain dimensions and the dependence of viscoelastic properties on concentration, molecular weight and solvent power, Polymer (Guildford) 21 (1980) 258–262, https://doi.org/10.1016/0032-3861(80)90266-9.
[78] L.E. Rodd, T.P. Scott, J.J. Cooper-White, G.H. McKinley, Capillary break-up rheometry of low-viscosity elastic fluids, Appl. Rheol. 15 (2005) 12–27, https://doi.org/10.1515/arh-2005-0001.
[79] S.H. Spiegelberg, D.C. Ables, G.H. McKinley, The role of end-effects on measurements of extensional viscosity in filament stretching rheometers, J. Nonnewton. Fluid Mech. 64 (1996) 229–267, https://doi.org/10.1016/0377-0257(96)01439-5.
[80] S.J. Haward, V. Sharma, C.P. Butts, G.H. McKinley, S.S. Rahatekar, Shear and extensional rheology of cellulose/ionic liquid solutions, Biomacromolecules 13 (2012) 1688–1699, https://doi.org/10.1021/bm300407q.
[81] M.S.N. Oliveira, R. Yeh, G.H. McKinley, Iterated stretching, extensional rheology and formation of beads-on-a-string structures in polymer solutions, J. Nonnewton. Fluid Mech. 137 (2006) 137–148, https://doi.org/10.1016/j.jnnfm.2006.01.014.
[82] M.A. Martín-Alfonso, J.F. Rubio-Valle, G.M. Estrada-Villegas, M. Sánchez-Domínguez, J.E. Martín-Alfonso, Exploring cellulose triacetate nanofibers as sustainable structuring agent for castor oil: formulation design and rheological insights, Gels 10 (2024) 221, https://doi.org/10.3390/gels10040221.
[83] J.F. Rubio-Valle, M.C. Sánchez, C. Valencia, J.E. Martín-Alfonso, J.M. Franco, Production of lignin/cellulose acetate fiber-bead structures by electrospinning and exploration of their potential as green structuring agents for vegetable lubricating oils, Ind. Crop. Prod. 188 (2022) 115579, https://doi.org/10.1016/j.indcrop.2022.115579.
[84] M.C. Sánchez, J.M. Franco, C. Valencia, C. Gallegos, F. Urquiola, R. Urchegui, Atomic force microscopy and thermo-rheological characterisation of lubricating greases, Tribol. Lett. 41 (2011) 463–470, https://doi.org/10.1007/s11249-010-9734-x.
[85] M.A. Delgado, M.C. Sánchez, C. Valencia, J.M. Franco, C. Gallegos, Relationship among microstructure, rheology and processing of a lithium lubricating grease, Chem. Eng. Res. Des. 83 (2005) 1085–1092, https://doi.org/10.1205/cherd.04311.